

Color Patterning of Luminescent Perovskites via Light-Mediated Halide Exchange with Haloalkanes

Ying-Chieh Wong, Wen-Bin Wu, Tian Wang, Jun De Andrew Ng, Khoong Hong Khoo,*
Jie Wu,* and Zhi-Kuang Tan*

Lead halide perovskite possesses a semiconductor bandgap that is readily tunable by a variation in its halide composition. Here, a photo-activated halide exchange process between perovskite nanocrystals and molecular haloalkanes is reported, which enables the perovskite luminescence to be controllably shifted across the entire visible spectrum. Mechanistic investigations reveal a mutual exchange of halogens between the perovskite crystal surface and a chemisorbed haloalkane, yielding nanocrystals and haloalkanes with mixed halide contents. Exchange kinetics studies involving primary, secondary, and tertiary haloalkanes show that the rate of reaction is governed by the activation barrier in the breakage of the covalent carbon–halogen (C–X) bond, which is a function of the C–X bond energy and carbon radical stability. Employing this halide exchange approach, a micrometer-scale trichromatic patterning of perovskites is demonstrated using a light-source-integrated inkjet printer and tertiary haloalkanes as color-conversion inks. The haloalkanes volatilize after halide exchange and leave no residues, thereby offering significant processing advantage over conventional salt-based exchange techniques. Beyond the possible applications in new-generation micro-LED and electroluminescent quantum dot displays, this work exemplifies the rich surface and photochemistry of perovskite nanocrystals, and could lead to further opportunities in perovskite-based photocatalysis and photochemical sensing.

Lead halide perovskite semiconductors have, in the recent years, emerged very successful in photovoltaic^[1–5] and light-emitting device^[6–16] applications. They stand out from other conventional semiconductors due to their easy solution-processing and their

facile bandgap tuning. Earlier works on photovoltaics rely on lead iodide and lead bromide based perovskites to achieve devices with different light-absorption profile and open-circuit voltages.^[1,17] However, the true benefit of bandgap tuning is realized in light-emitting devices, where strong and narrow line-width emission can be conveniently produced across an extensive ultraviolet to visible to near-infrared spectral region.^[6,18]


The tailoring of perovskite bandgap and light-emission profile is typically achieved through the variation of halides (i.e., chloride, bromide, or iodide) in the chemical precursors, or via postsynthetic halide exchange. Various strategies for halide exchange have been reported in the literature,^[19–22] and are typically attributed to a direct exchange of anionic halide species. Here, we report a photo-activated halide exchange process between cesium lead halide perovskite nanocrystals and a variety of molecular haloalkanes to achieve full spectral tuning in the visible region. We show, through detailed mechanistic studies, that this process is surface-mediated and involves the photo-activated breakage of

covalently linked carbon–halogen bonds. This is consistent with our earlier reports, where we show that perovskite nanocrystals are capable of performing surface-mediated photocatalytic reactions.^[23,24] Crucially, we demonstrate that our halide exchange approach could be employed in the micrometer-sized patterning of perovskite films to achieve trichromatic light emission, which has important utility in the manufacturing of functional color displays.

We prepared luminescent cesium lead bromide (CsPbBr₃) nanocrystals following literature-reported methods,^[25] and dispersed the nanocrystals into dichloromethane (DCM) solvent. We added 0.007 M of thiophenol into the solution, which we show in our previous work^[23] is capable of enhancing the photoluminescence (PL) of the perovskite nanocrystals. The solution was then illuminated with a coiled white LED strip (1 m, 9 W). The reaction progress was tracked by extracting aliquots of the reaction mixture at timed intervals, followed by the measurement of their PL spectra.

As shown in **Figure 1a**, the PL of the nanocrystal solutions blueshifted monotonically from 523 nm (green) at 0 h to 447 nm (blue) at 8 h. This observation suggests that the bromide ions in CsPbBr₃ were progressively replaced by chloride

Dr. Y.-C. Wong, W.-B. Wu, T. Wang, J. D. A. Ng,
Prof. J. Wu, Prof. Z.-K. Tan
Department of Chemistry
National University of Singapore
3 Science Drive 3, Singapore 117543, Singapore
E-mail: chmjie@nus.edu.sg; chmtanz@nus.edu.sg
J. D. A. Ng, Prof. Z.-K. Tan
Solar Energy Research Institute of Singapore
National University of Singapore
7 Engineering Drive 1, Singapore 117574, Singapore
Dr. K. H. Khoo
Institute of High Performance Computing
1 Fusionopolis Way, Singapore 138632, Singapore
E-mail: khookh@ihpc.a-star.edu.sg

 The ORCID identification number(s) for the author(s) of this article can be found under <https://doi.org/10.1002/adma.201901247>.

DOI: 10.1002/adma.201901247

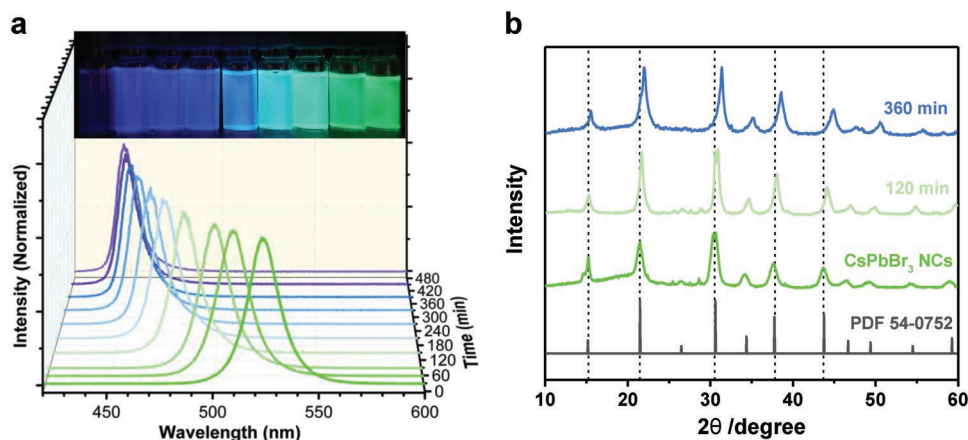


Figure 1. a) Normalized PL spectra showing the spectral shifts of perovskite nanocrystals in reaction mixtures comprising CsPbBr₃ in DCM. Inset image shows photoluminescence of the reaction mixtures under 365 nm UV excitation. b) XRD spectra of CsPbBr₃ in DCM, showing changes in the perovskite lattice spacing.

ions, causing the bandgap to widen and the PL of the nanocrystals to blueshift. This halide exchange process slows down significantly over time, and the PL shifts negligibly after 8 h. An equilibrium concentration of bromide and chloride is likely to be established in both the solution and the nanocrystals at the end of the reaction, hence preventing a complete exchange to give pure chloride CsPbCl₃ nanocrystals. The PL quantum yield changed slightly from 61% to 51% after 8 h, thereby suggesting that the photo-activated reaction does not introduce much defects to the nanocrystals.

To provide further evidence toward a halide exchange, we performed X-ray diffraction (XRD) studies on the perovskite nanocrystals before and after photo-illumination (see Figure 1b), and observed a monotonic shift in the diffraction patterns toward larger angles. This is a clear indication of a reduction in lattice spacing from 0.583 to 0.570 nm, as would be expected for a halide change from larger bromide to smaller chloride ions.

Transmission electron microscopy (TEM) images of the perovskite crystals before and after the reaction showed a slight decrease in crystal size from 10.8 ± 1.7 to 9.7 ± 1.5 nm (see Figure 2a,b), which is likely due to the reduction in lattice constant. The shape or morphology of the nanocrystals remains unchanged after the halide exchange reaction. We further measured the halide composition of the nanocrystals using energy-dispersive X-ray spectroscopy (EDX; Figure S1, Supporting Information), and results confirm that a halide change from bromide to chloride has indeed occurred.

For control studies, we conducted the experiments in the dark and verified that there were no spectral shifts in the perovskite, indicating that this halide exchange reaction with dichloromethane was photo-activated. We also performed the experiments in the absence of PL-enhancing thiophenol and observed the same PL spectral blueshift (see Figure S2, Supporting Information), hence confirming that the additive did not play a role in the halide exchange process.

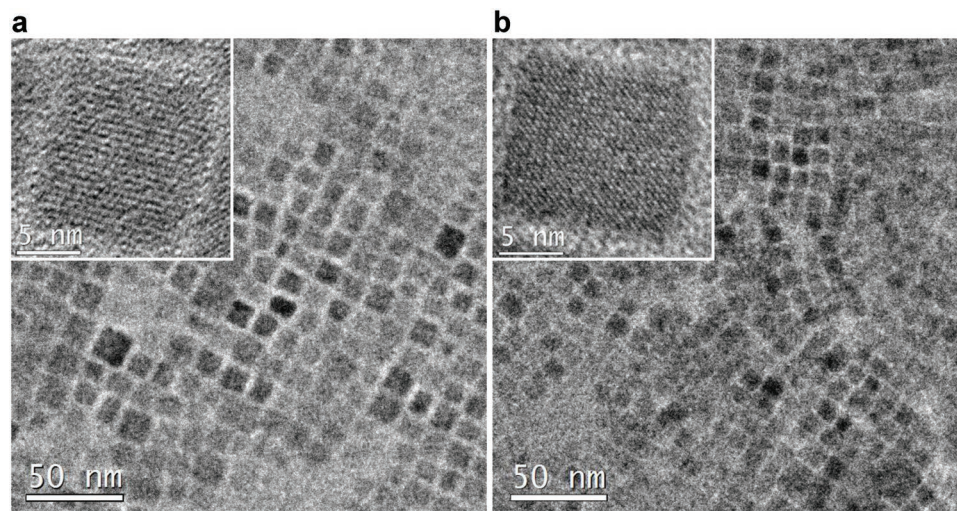


Figure 2. a,b) TEM images of CsPbBr₃ nanocrystals in DCM before (a) and after (b) 8 h light irradiation. The inset contains high-resolution TEM images of the corresponding samples.

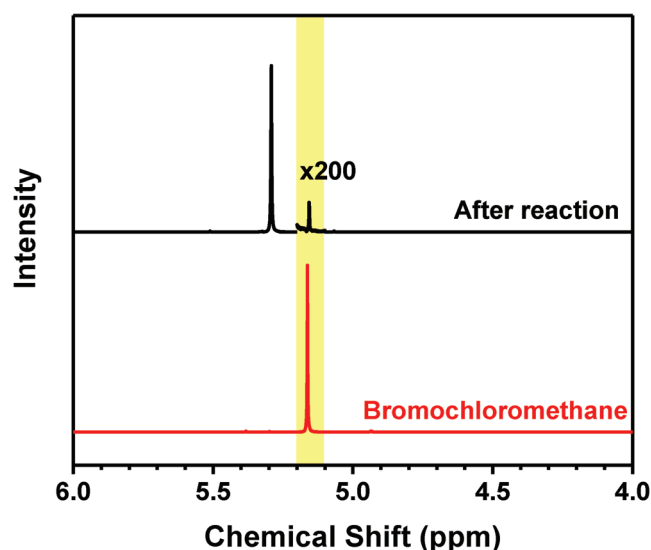


Figure 3. ^1H -NMR spectrum of haloalkane (dichloromethane) after halide exchange reaction. The section highlighted in yellow is multiplied by 200 \times . A reference spectrum of bromochloromethane is shown in red.

A halide exchange reaction should involve a mutual swap of halides on both the perovskite nanocrystals and the haloalkane. We measured the proton nuclear magnetic resonance (^1H NMR) spectra of the reaction product mixture, and found that a portion of the dichloromethane has indeed been converted to bromochloromethane. The ^1H NMR spectra in **Figure 3** show the appearance of a signal at δ 5.16 ppm after reaction, which is characteristic of bromochloromethane, hence confirming that a mutual halide exchange has occurred.

In order to test if an exchange reaction from bromide to iodide was possible, we performed the experiment with iodo-propane added to the reaction mixture. As shown in **Figure 4**, the PL shifted from 505 nm (cyan) to 620 nm (red), indicating an incremental replacement of bromide with iodides. The PL quantum yield decreased slightly from 61% to 40% after the iodide exchange reaction. The XRD spectra in **Figure S3** in the Supporting Information show the resulting decrease in scattering angles, indicative of an increase in lattice spacing from 0.583 to 0.601 nm due to the bromide–iodide exchange. We note that a much smaller concentration of iodoalkane was sufficient to elicit a bromide–iodide exchange, compared to the bromide–chloride exchange with dichloromethane. This is because the carbon–iodide bond is significantly weaker and easier to break compared to the carbon–chloride bond.

To gain deeper insights into the mechanistic pathways of the halide exchange reaction, we performed two sets of experiments involving the bromide-to-iodide and iodide-to-bromide halide exchange between perovskite nanocrystals and the corresponding of primary (1-propyl), secondary (2-propyl), and tertiary (*t*-butyl) haloalkanes. The halide exchange dynamics are shown in **Figure 4**, and a few key trends could be observed: 1) Halide exchange involving bromoalkane is slower than those involving the corresponding iodoalkane. This indicates that the rate-determining step involves the breakage of carbon–halogen (C–X) bond, where C–Br bond is stronger than C–I bond. 2) Reaction was slightly faster for the secondary haloalkane

compared to the primary haloalkane. 3) All tertiary haloalkane reactions are rapid. These are attributable to the stabilization of the carbon radical intermediate generated during the C–X bond breakage, where the tertiary carbon radical is stabilized by hyperconjugation to a significant extent and the secondary and primary carbon radical is stabilized to a lesser extent.

The above results suggest that the activation barrier height is determined by the C–X bond energy and the carbon radical stabilization, and that the surmounting of this barrier by photon energy is required for the halide exchange reaction to proceed. It is also clear that the halide exchange is not a $\text{S}_{\text{N}}2$ -type reaction where a halide ion is ejected from the perovskite surface and subsequently undergoes a nucleophilic attack of the haloalkane, since the primary haloalkanes would be most reactive if that were the case. It is also worth noting that the reaction is not a typical $\text{S}_{\text{N}}1$ reaction involving the spontaneous breakage of the C–X bond since photo-activation of the perovskite is required for reaction, hence indicating that the reactive precursor must involve a perovskite-coupled haloalkane species.

Based on the above-accumulated experimental evidence, we propose a vacancy defect facilitated reaction mechanism which comprises the five major states shown in **Figure 5a**. Going from left to right, we have: 1) Haloalkane approaches a perovskite solid surface that contains a halogen vacancy. 2) Halogen on haloalkane coordinates with Pb at the vacancy to form a lead–halogen bond. 3) Carbon–halogen bond breaks to form a carbon radical. 4) Carbon radical migrates and bonds with a neighboring halogen on the surface. 5) The new haloalkane molecule leaves the surface, re-forming the vacancy defect. The orientations of the surface-attached haloalkane in steps (2) and (4) are determined by the shape of lowest occupied molecular orbitals (LUMO) of the haloalkanes, as shown in **Figure S4** in the Supporting Information.

First-principles density functional theory (DFT) calculations were performed to determine the relative energies for each step of the proposed pathway to verify the plausibility of the proposed mechanism and the involvement of light in this reaction. **Figure 5b–d** shows the ground state (in blue) and excited state (in red) energy-level diagrams of CsPbBr_3 -iodoalkane exchange reaction for the primary, secondary, and tertiary systems, respectively, while **Figure 5e–g** shows the corresponding diagrams of CsPbI_3 -bromoalkane exchange reaction. In the excited-state calculations, we introduced an additional electron into the system to simulate the photo-excitation and the resulting occupation of the conduction band or LUMO.

For the primary and secondary haloalkane systems, the energy barrier between the ground states of steps (2) and (3), which corresponds to C–X bond breaking, is the highest and therefore points to the rate-determining step of the halide exchange reaction. The corresponding barrier for the excited state is significantly lowered, hence indicating that photo-excitation can be effective in promoting the C–X bond-breaking process. It is also clear from the calculations that the C–Br bond-breaking barriers are consistently larger than the C–I bond-breaking barriers, hence accounting for the slower reactions involving the bromoalkane. The activation barriers for the secondary systems are calculated to be smaller than that for the primary systems, hence accounting for the faster reactions in the secondary systems. In the cases involving the tertiary

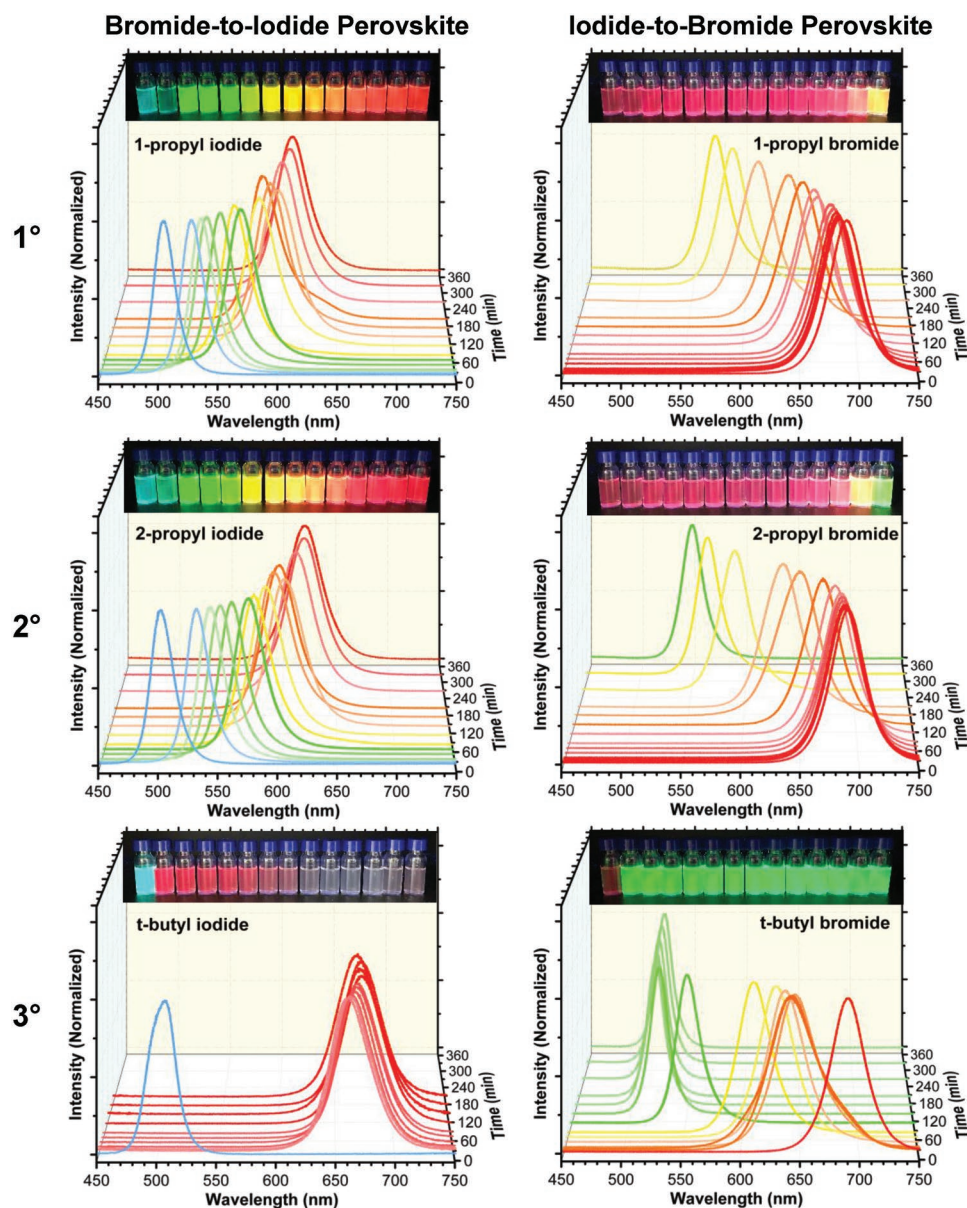


Figure 4. Comparison of bromide-to-iodide and iodide-to-bromide halide exchange between perovskite nanocrystals and the corresponding primary (1-propyl), secondary (2-propyl), and tertiary (*t*-butyl) haloalkanes.

haloalkanes, the ground-state and excited-state activation barriers for C–X bond breaking are small, hence explaining the rapid halide exchange reactions. In general, the DFT calculations for our proposed halide exchange mechanistic pathway are consistent with our experimental findings.

To demonstrate the utility of our halide exchange process, we printed a pattern of our university logo using green-emitting CsPbBr₃ perovskite nanocrystals, and converted portions of the logo to emit in red and blue, using a light-source-integrated Dimatix inkjet printer and the corresponding haloalkanes as inks. The resulting trichromatic logo, achieved through this halide exchange color-patterning approach, is shown in **Figure 6a**. *Tert*-butyl chloride and *tert*-butyl iodide were employed, respectively, as precursors to the blue and red

perovskites, due to their rapid halide exchange capabilities as shown in our kinetics studies above. Figure 6b shows that the smallest dimensions achievable using our methods and equipment are in the order of 50 μm , which is an excellent resolution for most display applications. We note that the haloalkanes vaporize soon after the exchange process and do not leave behind any residues on the perovskite thin film. This offers significant advantage over other salt-based halide exchange methods, where remnants of the exchanged salts may cause undesirable haze or potential reverse-exchange issues. We envision that our convenient post-deposition color-conversion approach could be useful in new-generation color-conversion micro-LED displays or electroluminescent quantum dot displays where micropatterned trichromatic light emission is required.

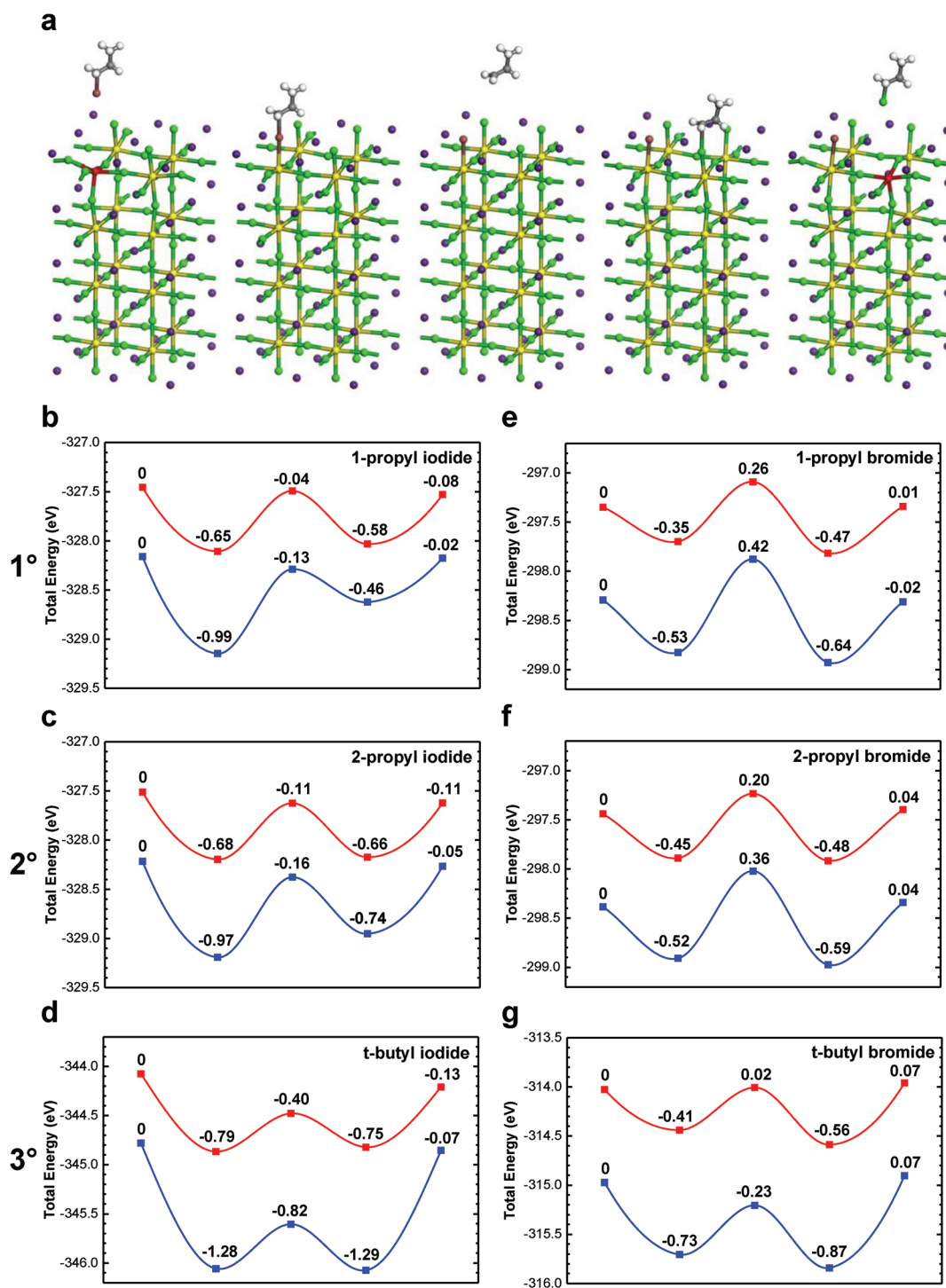


Figure 5. a) Halide exchange reaction mechanism between perovskite (001) surface and representative haloalkane (red: Pb at vacancy defect; yellow: Pb; purple: Cs; gray: C; green: Br; brown: I; white: H). b–d) Ground-state (in blue) and excited-state (in red) energy-level diagram of CsPbBr₃-iodoalkane exchange reaction, and e–g) corresponding energy-level diagram of CsPbI₃-bromoalkane exchange reaction. The number at each data point represents the energy relative to the first step in eV.

In addition to the relevant applications in the commercial display industry, this work also offers rich insights into the surface activity of perovskite nanocrystals, having shown that strong carbon–halogen bonds, such as C–Cl and C–Br bonds,

can be broken and re-formed using mild, surface-mediated photo-activation pathways. This sets the stage toward the use of lead halide perovskites for interesting new applications in photocatalysis and in photochemical sensing.

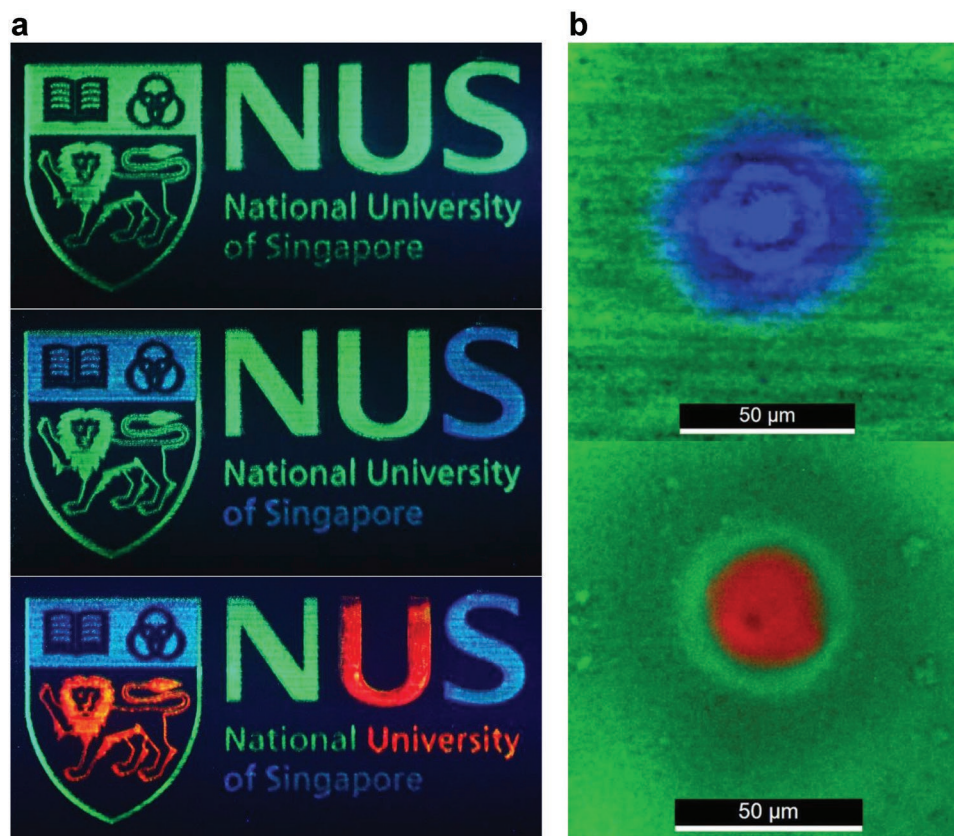


Figure 6. a) Step-by-step fast halide exchange between green-emitting CsPbBr₃ nanocrystals and inkjet-printed *tert*-butyl chloride and *tert*-butyl iodide haloalkanes to give a trichromatic university logo. b) Fluorescence microscopy images showing 50 µm sized blue and red dots achievable through halide exchange with haloalkanes.

Supporting Information

Supporting Information is available from the Wiley Online Library or from the author.

Acknowledgements

Y.-C.W., W.-B.W., T.W., and J.D.A.N. contributed equally to this work. The authors are grateful for the financial support provided by the Ministry of Education of Singapore and the National University of Singapore (R-143-000-639-133, R-143-000-674-114, R-143-000-691-114 and R-143-000-A10-133, R-143-000-A30-112). K.H.K. would like to thank Dr. R. Laskowski for helpful discussions. The authors also thank the National Supercomputing Center, Singapore, for providing computational resources. The authors declare no competing financial interests.

Conflict of Interest

The authors declare no conflict of interest.

Keywords

color patterning, displays, halide exchange, nanocrystals, perovskites

Received: February 23, 2019
Revised: April 1, 2019
Published online: April 22, 2019

- [1] A. Kojima, K. Teshima, Y. Shirai, T. Miyasaka, *J. Am. Chem. Soc.* **2009**, *131*, 6050.
- [2] M. M. Lee, J. Teuscher, T. Miyasaka, T. N. Murakami, H. J. Snaith, *Science* **2012**, *338*, 643.
- [3] H.-S. Kim, C.-R. Lee, J.-H. Im, K.-B. Lee, T. Moehl, A. Marchioro, S.-J. Moon, R. Humphry-Baker, J.-H. Yum, J. E. Moser, M. Grätzel, N.-G. Park, *Sci. Rep.* **2012**, *2*, 591.
- [4] J. Burschka, N. Pellet, S.-J. Moon, R. Humphry-Baker, P. Gao, M. K. Nazeeuruddin, M. Grätzel, *Nature* **2013**, *499*, 316.
- [5] N. J. Jeon, J. H. Noh, Y. C. Kim, W. S. Yang, S. Ryu, S. I. Seok, *Nat. Mater.* **2014**, *13*, 897.
- [6] Z.-K. Tan, R. S. Moghaddam, M. L. Lai, P. Docampo, R. Higler, F. Deschler, M. Price, A. Sadhanala, L. M. Pazos, D. Credgington, F. Hanusch, T. Bein, H. J. Snaith, R. H. Friend, *Nat. Nanotechnol.* **2014**, *9*, 687.
- [7] J. Wang, N. Wang, Y. Jin, J. Si, Z.-K. Tan, H. Du, L. Cheng, X. Dai, S. Bai, H. He, Z. Ye, M. L. Lai, R. H. Friend, W. Huang, *Adv. Mater.* **2015**, *27*, 2311.
- [8] G. Li, Z.-K. Tan, D. Di, M. L. Lai, L. Jiang, J. H.-W. Lim, R. H. Friend, N. C. Greenham, *Nano Lett.* **2015**, *15*, 2640.
- [9] H. Cho, S.-H. Jeong, M.-H. Park, Y.-H. Kim, C. Wolf, C.-L. Lee, J. H. Heo, A. Sadhanala, N. Myoung, S. Yoo, S. H. Im, R. H. Friend, T.-W. Lee, *Science* **2015**, *350*, 1222.
- [10] G. Li, F. W. R. Rivarola, N. J. L. K. Davis, S. Bai, T. C. Jellicoe, F. de la Peña, S. Hou, C. Ducati, F. Gao, R. H. Friend, N. C. Greenham, Z.-K. Tan, *Adv. Mater.* **2016**, *28*, 3528.
- [11] M. Yuan, L. N. Quan, R. Comin, G. Walters, R. Sabatini, O. Voznyy, S. Hoogland, Y. Zhao, E. M. Beauregard, P. Kanjanaboos, Z. Lu, D. H. Kim, E. H. Sargent, *Nat. Nanotechnol.* **2016**, *11*, 872.

- [12] N. Wang, L. Cheng, R. Ge, S. Zhang, Y. Miao, W. Zou, C. Yi, Y. Sun, Y. Cao, R. Yang, Y. Wei, Q. Guo, Y. Ke, M. Yu, Y. Jin, Y. Liu, Q. Ding, D. Di, L. Yang, G. Xing, H. Tian, C. Jin, F. Gao, R. H. Friend, J. Wang, W. Huang, *Nat. Photonics* **2016**, *10*, 699.
- [13] Z. Xiao, R. A. Kerner, L. Zhao, N. L. Tran, K. M. Lee, T.-W. Koh, G. D. Scholes, B. P. Rand, *Nat. Photonics* **2017**, *11*, 108.
- [14] K. Lin, J. Xing, L. N. Quan, F. P. García de Arquer, X. Gong, J. Lu, L. Xie, W. Zhao, D. Zhang, C. Yan, W. Li, X. Liu, Y. Lu, J. Kirman, E. H. Sargent, Q. Xiong, Z. Wei, *Nature* **2018**, *562*, 245.
- [15] Y. Cao, N. Wang, H. Tian, J. Guo, Y. Wei, H. Chen, Y. Miao, W. Zou, K. Pan, Y. He, H. Cao, Y. Ke, M. Xu, Y. Wang, M. Yang, K. Du, Z. Fu, D. Kong, D. Dai, Y. Jin, G. Li, H. Li, Q. Peng, J. Wang, W. Huang, *Nature* **2018**, *562*, 249.
- [16] X. Zhao, J. D. A. Ng, R. H. Friend, Z.-K. Tan, *ACS Photonics* **2018**, *5*, 3866.
- [17] J. H. Noh, S. H. Im, J. H. Heo, T. N. Mandal, S. I. Seok, *Nano Lett.* **2013**, *13*, 1764.
- [18] G. Xing, N. Mathews, S. S. Lim, N. Yantara, X. Liu, D. Sabba, M. Grätzel, S. Mhaisalkar, T. C. Sum, *Nat. Mater.* **2014**, *13*, 476.
- [19] D. M. Jang, K. Park, D. H. Kim, J. Park, F. Shojaei, H. S. Kang, J.-P. Ahn, J. W. Lee, J. K. Song, *Nano Lett.* **2015**, *15*, 5191.
- [20] G. Nedelcu, L. Protesescu, S. Yakunin, M. I. Bodnarchuk, M. J. Grotevent, M. V. Kovalenko, *Nano Lett.* **2015**, *15*, 5635.
- [21] Q. A. Akkerman, V. D'Innocenzo, S. Accornero, A. Scarpellini, A. Petrozza, M. Prato, L. Manna, *J. Am. Chem. Soc.* **2015**, *137*, 10276.
- [22] D. Parobek, Y. Dong, T. Qiao, D. Rossi, D. H. Son, *J. Am. Chem. Soc.* **2017**, *139*, 4358.
- [23] W.-B. Wu, Y.-C. Wong, Z.-K. Tan, J. Wu, *Catal. Sci. Technol.* **2018**, *8*, 4257.
- [24] Y.-C. Wong, J. De Andrew Ng, Z.-K. Tan, *Adv. Mater.* **2018**, *30*, 1800774.
- [25] L. Protesescu, S. Yakunin, M. I. Bodnarchuk, F. Krieg, R. Caputo, C. H. Hendon, R. X. Yang, A. Walsh, M. V. Kovalenko, *Nano Lett.* **2015**, *15*, 3692.